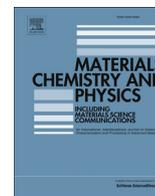




Contents lists available at ScienceDirect

Materials Chemistry and Physics

journal homepage: www.elsevier.com/locate/matchemphys

High entropy alloys obtained by field assisted powder metallurgy route: SPS and microwave heating

E. Colombini ^{a,*}, R. Rosa ^a, L. Trombi ^a, M. Zadra ^b, A. Casagrande ^c, P. Veronesi ^a

^a Department of Engineering “Enzo Ferrari”, via Vivarelli 10/1, 41125 Modena, Italy

^b K4Sint, via Dante 300-B.I.C., Pergine Valsugana, Italy

^c Department of Industrial Engineering, viale Risorgimento 4, 40136 Bologna, Italy

HIGHLIGHTS

- Innovative microwave synthesis of high entropy alloys starting from metal powder.
- Comparison between two different powder metallurgy technique.
- Numerical simulation to gain a deeper understanding of the reaction.

ARTICLE INFO

Article history:

Received 1 April 2017

Received in revised form

28 June 2017

Accepted 30 June 2017

Available online xxx

Keywords:

Microwaves

High entropy alloy (HEA)

Powder metallurgy

Simulation

ABSTRACT

The aim of this work was to investigate the field assisted powder metallurgy route for producing HEAs at equimolar composition, i.e. FeCoNiCrAl, starting from metal powders. Both mixed, mechanically activated and mechanically alloyed powders have been used. The powders obtained by mechanical alloying were synthesized only by SPS, whereas the remaining ones were sintered by SPS or microwave heating. The investigated field assisted sintering techniques allowed an extremely short alloying time, high energy density on the load and negligible contamination by the surrounding environment. Both the conducted sintering-synthesis technology resulted not definitive to produce chemical homogeneity and to obtain a single stable structure. Thus a subsequently heat treatment was required. The post heat treatment, indeed, led to a single crystalline structure (FCC) and the material was fully recrystallized. After heat treatment samples are isomorphic: they exhibit two different phases with the same FCC cell, but different chemical composition, in detail Fe-Cr richer and Al-Ni richer. SPS-ed samples present a reduced porosity, while microwave processed ones are much more porous and this is reflected in the mechanical properties.

© 2017 Elsevier B.V. All rights reserved.

1. Introduction

Since the introduction of the concept of high entropy alloys in 2004 [1,2] they have been attracting much attention across the world, due to their unique properties [3]. This new class of alloys, called also multi component alloys [4], where each one of the major elements has a concentration between 5 and 35 at% with high mixing entropy in their liquid state [5,6], can be tailored to enhance many promising properties, such as high hardness [7], wear resistance [8] excellent high and low-temperature strength [9–11] and in general good resistance to oxidation and corrosion [12].

According to the literature research [13–16,4] the most used processing routes for multi components alloy systems are:

- from the liquid state, e.g arc melting [17] and induction melting [18], where the obtained ingots are remelted under high vacuum at least three or four times to improve the homogeneity; more recently splat quenching [19], selective electron beam melting [20], laser [21,22] and direct laser (DLF) [13,16] technologies have been used as well
- from the solid state, using powder metallurgy, i.e. mechanical alloying [23] [24], spark plasma sintering [25]
- from the gas state, such as sputtering techniques, i.e magnetron sputtering [26], plasma deposition [13].
- by electrochemical process [27] (used mainly for coatings).

* Corresponding author.

E-mail address: elena.colombini@unimore.it (E. Colombini).

The alloys prepared from the liquid phase usually have many structural defects such as voids, porosity, and a generally low as-cast hardness [4]. Recently, further developments in the powder metallurgy route provided promising results [25,28] despite a higher pore density for samples produced by mechanical alloying (MA) followed by consolidation [29]. However, the solidification from the molten state is usually accompanied by micro-segregations, while by the MA process, more homogenous chemical distribution and solid solubility extension could be reached [15].

Hence, an ideal synthetic route to produce HEAs should guarantee short alloying time (achievable, for instance, applying high energy density on the load [28], leading to rapid melting [30] and reduced contamination by the surrounding environment), efficient cooling [31] and capability to operate in controlled atmosphere. Besides the aforementioned synthetic routes, such conditions can be achieved using high frequency electromagnetic fields, like in microwave heating [32], provided that the load is capable to couple with the incident electric and magnetic field. This technique belongs to the so called FAST - Field Assisted Sintering Techniques, like spark plasma sintering [33–35]. Scientific literature regarding the use of microwaves to prepare HEA is limited to few contributions [24,37,38], in which HEAs are prepared by microwave-assisted combustion synthesis, starting from oxidic precursors as raw materials (and hence having alumina as by product [34]) or by metallic powders mixtures [24,36–38]. Microwave assisted combustion synthesis of pure metal powders as reactants has already been used during last decade by some of the authors to prepare intermetallics [39], functionally graded materials [40], or to join dissimilar materials [41]. The advantage of applying microwaves to combustion synthesis reactions is the high purity of the products, the rapid ignition of the reaction [42], the possibility to control the products microstructure [43] and cooling rate after synthesis, especially in presence of ferromagnetic reactants [44]. When applied to HEA synthesis starting from metallic powders, such processing route allows the formation of a minimal fraction of liquid phase, thus leading to the possibility of achieving microwave assisted near-net-shape processing [24], able to overcome the limits of current melting technologies (defects formation) or conventional solid state ones (time demanding), but with the drawback of some residual porosity ascribable to the pressureless conditions used [37,38].

The aim of this study is to investigate the field assisted synthesis of FeCoNiCrAl starting from metal powders mixture and single phase formation obtained by subsequently heat treatment.

Among the several family of HEAs the FeCoNiCrAl has been selected for field assisted processing due to its peculiar precursors composition: at least one ferromagnetic element (Fe, Co, Ni) is present and a further heat contribution is expected during synthesis as a consequence of the presence of at least one highly reactive element couple, like Al-Ni, Al-Fe, Al-Co. Moreover, the use of Al is expected to have the synthesis initiated below 700 °C [37,45] roughly corresponding to the melting point of aluminum.

2. Materials and methods

The following elemental powders (Table 1), supplied by Sigma

Table 1
Composition of the metal powders used (BCC = body centered cubic; FCC = face centered cubic; HCP = Hexagonal close-packed arrangement).

Element	Purity (%)	Particle Size (µm)	Cell
Fe	97.00	<44	BCC
Co	99.80	<2	HCP
Ni	99.70	<5	FCC
Cr	99.00	<44	BCC
Al	99.00	<75	FCC

Aldrich, were exploited as reactants to prepare equiatomic FeCoCrNiAl.

Two different routes to prepare the powder mixture were exploited:

- mixing for 20 min to homogenize the powders;
- mechanical activation by high energy milling for 1
- mechanosynthesis (prealloying) by high energy milling for 35 h (an interval longer than 15 h is required to achieve the mechanical alloying [24,45].

Both mixing and the mechanical alloying were carried out using a Planetary Ball Mill PM 100 by Retsch GmbH, at 250 rpm in an argon atmosphere, with steel balls, BPR 10:1 and cycles of 20 min milling followed by 5 min as break time to avoid overheating of the mixture.

The powders obtained by mechanical alloying were synthesized only by SPS, whereas the remaining ones were sintered by SPS or microwave heating.

In microwave synthesis, uniaxial pressing was used at 400 MPa to form reactive disc-shaped specimens of 20 mm diameter and 10 g as weight. A single-mode applicator based on the rectangular waveguide geometry (WR340) was used. The central part of the applicator presents predominant electric field conditions, while the regions near the side walls correspond to predominant maximum magnetic field conditions, for loads of small dimensions and not introducing major perturbations. In order to avoid excessive oxidation, a constant Ar flux (20 NmL/min) was blown into the single-mode applicator during experiments. The applicator is powered by a magnetron generator (MKS-Alter, Reggio Emilia, Italy), with an output power level ranging from 100 to 800 W, connected to a three-port circulator and to a three-stub tuner (MKS-Alter). A shorting plunger installed on the other side of the rectangular applicator allows to controllably modify the electromagnetic field distribution along the cavity. Temperature during heating tests was monitored and recorded at 1-s intervals, for load positioned in the predominant electric field region, using an optical pyrometer (IKS-T14-09, Sitel control Srl, Milan, Italy). The thermal synthesis, occurring with a strong exothermal event, was stopped immediately after the ignition of the reaction, in order to avoid possible annealing effects due to extended exposure to microwaves or high temperature.

In SPS, the powders were sintered in a DR.SINTER[®] SPS1050 (Sumitomo Coal & Mining, now SPS Syntex, Inc.) apparatus with graphite punches and dies. All samples have cylindrical geometry with a height of 5 mm and a diameter of 20 mm. SPS was performed at a nominal maximum temperature of 1000 °C or 1250 °C (measured with a thermocouple inserted into a blind hole in the die wall), with a uniaxial pressure of 60 MPa. The heating rate was 100 °C/min up to 950 °C and 50 °C/min up to the set sintering temperature. The maximum temperature and pressure were held for 5 min, before allowing the furnace to cool to room temperature.

All samples, after the preliminary consolidation operations with microwaves and SPS technological processes, were annealed at 1200 °C for 50 h in a tubular furnace, into a reactor containing titanium-shavings as getters, to reduce oxidative effects. The heat treatment was performed to improve samples homogeneity, leading to the single-phase formation of FCC solid solution.

The crystal structure was characterized by X-ray diffractometer (X'Pert PRO - PANalytical) with Cu-K α radiation and the microstructure was observed using scanning electron microscopy (SEM/ESEM - Quanta200 - FEI and SEM/FEG Nova NanoSEM 450 - FEI), after metallurgical preparation and etching by FeCl₃+HCl solution. Instrumented nano indentation (CSM Instruments) was used to

perform depth-sensing nano-indentation tests on samples. A 50 mN force with linear loading/unloading rate of 150 mN/min was applied for 15 s. The indentations were performed using a Berkovich tip and the elastic modulus and equivalent Vickers hardness were calculated according to the Oliver and Pharr method [46]. Microhardness test (Wolpert group 402 MVD instrument, Vickers, Wilson Wolpert Instruments, Aachen, Germany) was carried out as well, using 1 kg load.

3. Results

3.1. Microwave heating

The X-ray diffraction patterns of precursors powders is shown in Fig. 1, showing that in case of mechanical alloying, the FCC structure was already identifiable. Mechanical activation for 1 h, in the investigated condition, did not alter the phases present in the original mixture.

After microwave processing, requiring less than 30 s, as discussed later, the resulting X-ray diffraction patterns, shown in Fig. 2, evidenced the presence of two different crystalline structures, BCC and FCC, where the former is a minority phase and the last is the main phase. These features reflect the metastable microstructure deriving from the rapid synthesis by microwave processing. This metastability is reflected by a gradient in chemical composition within the microstructure, as discussed later.

The post-annealed (HT) phases can be identified as a simple FCC solid solution with diffraction peaks at about 20, 44, 50, 75, 90°, exactly positioned as α -Cu or steel austenite. Fe, Cr, Ni and Co alloying elements are expected to solubilize in supersaturated HEAs solid solution, while Al is dissolved in FCC solid solution and does not influence significantly structure of lattice, but only causes an increase of elastic distortion [13,15,47,60].

Microstructural analysis of the HEAs obtained by microwave processing of mixed powders, shown in Fig. 3, evidences the presence of a continuous liquid phase (light grey) wetting the larger particles (dark grey). Hence, a multi-phase structure is revealed, as confirmed by X-ray diffraction, where the coexistence of FCC and BCC phase was reported. The subsequent heat treatment induced the formation of a much more extended and homogenous phase, as detected by the X-ray diffraction, where FCC phase is pointed out, but the presence of two compositionally different solid solutions, as determined from EDX analysis is evident. This corresponds also to a lack of chemical homogeneity,

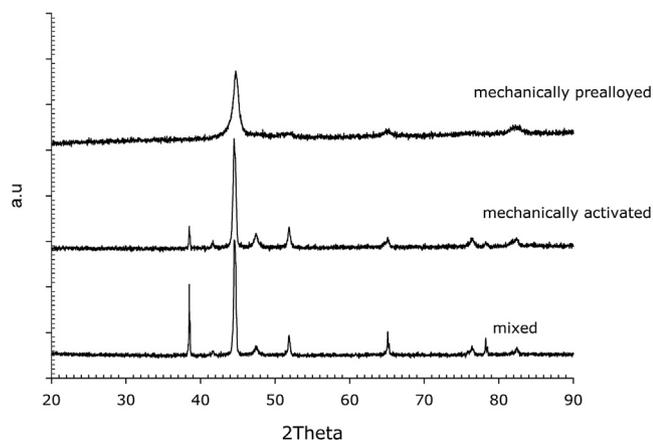


Fig. 1. X-ray diffraction pattern of powders precursors obtained by simple mixing, activation (1 h) or mechanical alloying (35 h).

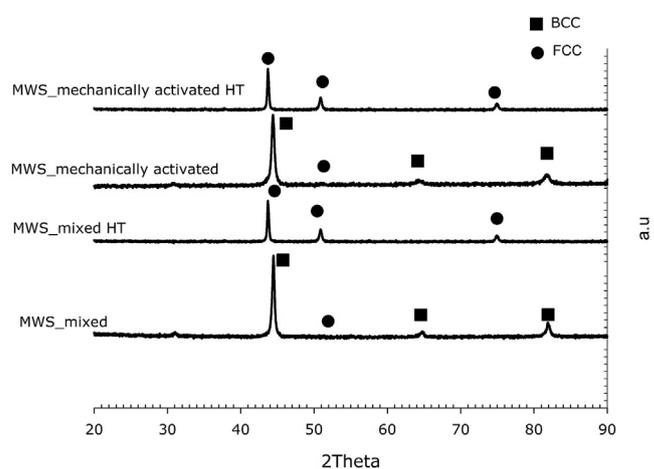


Fig. 2. X-ray diffraction pattern of microwave-processed HEA obtained by mixed powders or mechanically activated powders without or with (HT) post heat treatment.

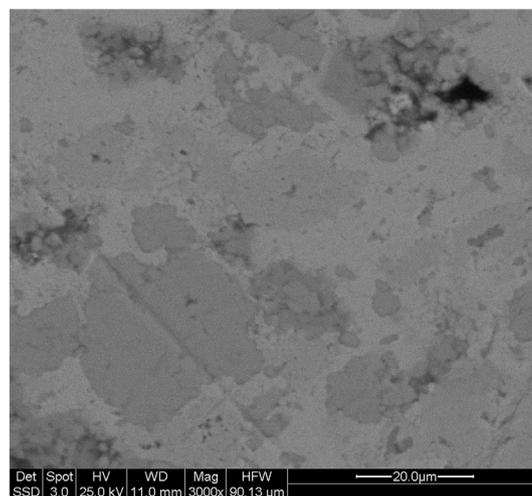


Fig. 3. SEM micrographs (backscattered electrons) of the microwave processed mixed powders.

as shown in Fig. 4, referred to post heat treated mechanically activated powders. Fig. 4 shows also that the mechanical activation led to much more homogenous results, as demonstrated by the presence of an extended phase with similar chemical composition.

Hence, microwave assisted synthesis of HEA starting from metallic powders mixtures proved to be, on one hand, extremely fast in the synthesis for the presence of liquid phases, but, on the other hand, it resulted somehow “slow” in the solid state synthesis [49]. Recently it was proposed that the diffusion and phase transformation kinetics in HEAs are slower than those in conventional processes [48]. Indeed, due to the equiatomic composition of this alloy, it is very likely that in the HEA lattice the neighboring atoms are of different nature, with different diffusion coefficient, which leads to different bonding in local atomic configuration. Thus, when performing rapid microwave assisted synthesis, this slower diffusion is expected to lead to the formation of metastable phases. So, in this study the post heat treatment is used to reactivate the diffusion, leading to the formation of stable phases, for example the unique FCC solid solution. This is also reflected in the

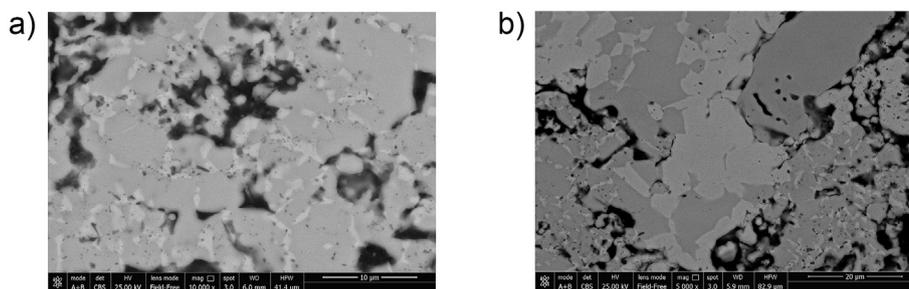


Fig. 4. SEM micrographs (backscattered electrons) of post heat treated samples obtained starting from mixed (a) or mechanically activated (b) powders.

X-ray diffraction measures (Fig. 2) where the as-synthesized mixed BCC/FCC structure was replaced by a post-annealed FCC one.

3.2. Microwave heating simulation

In the past, a predictive model of microwave ignited and sustained combustion synthesis of metal powder compacts, e.g NiAl, was developed by the authors [41,49–51]. In this framework, numerical simulation can be used to gain a deeper understanding of the reaction taking place extremely rapidly and volumetrically, for instance estimating temperature data otherwise difficult to be measured experimentally. The numerical simulation of the microwave assisted synthesis of HEA powders precursor compact was performed using the commercial software Comsol Multiphysics 3.3a. The multi-physics model simulating the microwave assisted synthesis was simplified to allow to reduce simulation time and lack of reliable data of dielectric properties of powder mixture as a function of temperature. Despite the assumption of no shape change of reactants and no temperature dependence of their dielectric and magnetic properties, the model allowed to gather a deeper insight to the microwave synthesis of powder compacts.

The numerical simulation requires to couple an electromagnetic model (RF application mode) with a chemical model which was necessary to study the reaction between powders and to account for a further heat generation term (reaction enthalpy). The electromagnetic part of the model was based on a prismatic microwave applicator (TE10n), built on the WR-340 waveguide geometry, which reproduced the experimental setup described previously, and sketched in Fig. 5.

This configuration well reflects the experimental set-up in which the same aim was reached by using a three-stub tuner (moving only one stub) and a shorting plunger.

The reaction to form the HEA was realized considering the following one single step reaction



This allows for a bi-directional coupling of thermal and radio-frequency aspects of the problem, via the average power density in the load, which is used to compute the temperature distribution in the load (pressed powders pellet), which, in turn, affects their electrical and dielectric properties.

The disc-shaped sample was placed in maximum electric field region. This configuration allows attaining rapid ignition condition in comparison with maximum magnetic field configuration. Rosa et al. [49] demonstrated that for each one of the intermetallic systems investigated (Fe, Co, Ni aluminides) ignition in predominant magnetic field resulted in lower amounts of heat generated in the reactive specimen to reach ignition, with respect to the values obtained when the ignition was reached in predominant E field. This was ascribed to a reduction in the amount of the reactive volume reaching ignition conditions, rather than on specific field-related effects.

Perfect electric conductor was chosen as boundary conditions for external walls of the waveguide, while in the microwave inlet port was set at a sinusoidal 2.45 GHz excitation in the TE10 mode. Heat generated by microwaves is used as input value to modify diffusion coefficients and to activate HEA powders mixture.

The reaction was described using the pre-defined Comsol Reaction Lab module. The module require kinetic parameters such as Arrhenius pre-exponential factors, A, and the activation energy E, as well as thermodynamic (e.g. entropy [J/(mol·K)], enthalpy [kJ/mol] and specific heat [J/kgK]) and physical data (concentration [mol/m³], density [kg/m³] and molecular weight). Pre-exponential factor and the activation energy were calculated by Kissinger

Table 2
Kinetic and thermodynamic parameters.

Reaction	A	E [kJ mol ⁻¹]	H [kJ mol ⁻¹] [50]	S [J mol ⁻¹ K ⁻¹] [50]
FeCoNiCrAl	677.4	182.5 E3	-12.32 E3	13.38

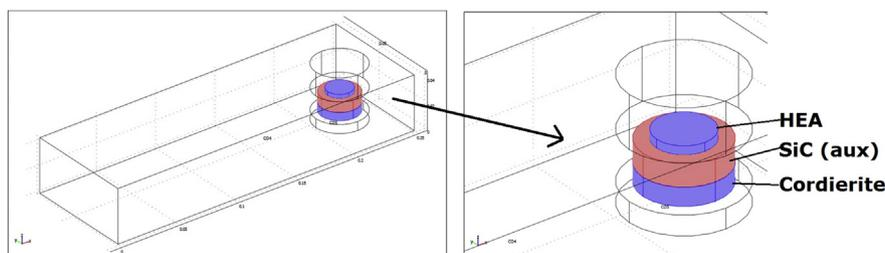


Fig. 5. Geometry model.

Table 3
Cp and starting concentration of species.

Element	[J mol ⁻¹ K ⁻¹]	C ₀ [mol/m ³]
Fe	25.10	29434.4
Co	24.81	29439.1
Ni	26.07	29439.1
Al	24.4	29439.1
Cr	23.35	29439.1
FeCoNiCrAl	24.75	0

method [52,53], by DSC measurement on NETZSCH STA 429 (CD) range 0.0/5.00 (K/min)/1400, at three different heating rate, i.e. 10 °C/min, 20 °C/min and 30 °C/min. Table 2 shows these data with relevant references, where available.

Concentration (Table 3) was calculated by stoichiometry, according to real geometric dimension obtained measuring a powder compact produced in laboratory according to the procedure described in the next section.

Due to the lack of reliable high temperature data on magnetic and dielectric properties of reactants and products at 2.45 GHz frequency, the electromagnetic part of the model referred to the reactants has been solved independently on the thermal one, in stationary conditions, in order to calculate the power density generated into the load by microwave-matter interaction and to be used as input in the heat transfer equation. The remaining parts of the model, instead, had temperature-dependent properties, like resistivity and thermal conductivity and a two-way coupled model was needed.

The reactants and product concentration variations during synthesis, obtained by the chemical model simulation, are shown in Fig. 6. From the chemical module, three values were exported i.e. reaction rate, concentration variation and heat source of reaction. The first two values were imported in the diffusion module while the third value (i.e. heat developed by the HEA) was employed into the heat transfer module. The RF module was then included and implemented into the model in order to furnish the necessary heat to ignite the synthesis.

In case of the precursors disc shaped domain, the heat source value is made up of reaction synthesis heat (exported from the chemical part of the model) and microwave heating source, as an inner volumetric heat source. Being the reactive powders and the

auxiliary SiC element the only microwave absorbing materials, only their contribution is used as heat source; for all other components the heat source is zero, due to microwave heating selectivity. Results obtained by the complete model are shown in Fig. 7 where the electric field distribution [Vm⁻¹] and resistive heating [W/m³] is reported. The plot shows that the reactive powders sample is volumetrically heated by microwaves, and that this heating occurs not completely homogeneously in the load. Hence, ignition is expected to occur at one side of the disc shaped sample, and not in the volume (i.e. not in thermal explosion regime), then propagating at the surrounding regions (SHS mode). Fig. 8 shows the simulated and measured temperature evolution plot of the central point of the load, from room temperature up to the adiabatic temperature of the reaction. Simulated results, despite the simplified model implemented, are in satisfactory agreement with the experimental values. It is possible to notice the rapid temperature increase, occurring when the microwave power generated into the load increases the temperature of the reactive specimen up to the ignition temperature. In the fully coupled model, it is possible to describe components cooling in order to obtain reliable temperature distributions of the system components.

3.3. SPS processing technique

Among the available metallic powder consolidation process, Spark Plasma Sintering is an innovative and recent technique which, in the case of metallic powder, implies an uni-axial pressure for the compaction, a simultaneous use of an electric current which passes through the compacted sample and promotes a direct joule heating effect [54]. In a similar manner to microwave heating, this technique promotes faster thermal cycles than for the usual melting and alloying of each metal at the time and conventional pressure assisted sintering during densification [55].

Fig. 9 shows the XRD patterns of the FeCoNiCrAl obtained by the SPS techniques at different temperature (i.e. 1000 °C and 1250 °C) and with different precursors preparation (mixed, mechanically activated, mechanically prealloyed). All samples after sintering exhibit the mixed FCC/BCC structure which is encountered also in literature [56,57].

The microstructure, shown in Fig. 10, presents a lack of compositional homogeneity, ascribable to the fast consolidation and synthesis, similarly to what obtained by microwave heating. Microstructural observations by SEM, evidenced the presence of regions rich in Al-Ni (BCC) close to regions richer in Fe-Cr (FCC) [58].

Noticeably, there are no evident pores, due to the pressure-assisted sintering technique used. The use of mechanically prealloyed powders and high temperature SPS provided the better homogeneity of the resulting HEA, despite the persistence of some partially reacted Cr particles, probably ascribable to their larger particles size (see Table 1).

The X-ray diffraction patterns after heat treatment are shown Fig. 11 and they demonstrate that only in case of pre-alloyed powders it was possible to achieve a single phase HEA. In all other cases, at the contrary of what happened using microwave synthesis, the BCC phase remained, independently on the maximum temperature used during SPS. This different behaviour could be ascribed to the different temperature distribution occurring during microwave or SPS processing. It is known [59] that when microwave processing metallic powders loads, arcing occurs among the particles, leading to an extremely high localized overheating, hic is not measured by the much larger sapphire fiber probe. Hence, microwave processing, despite the generally lower temperature measured, could lead to a better starting homogeneity due to this overheating effect, and thus a better response to post

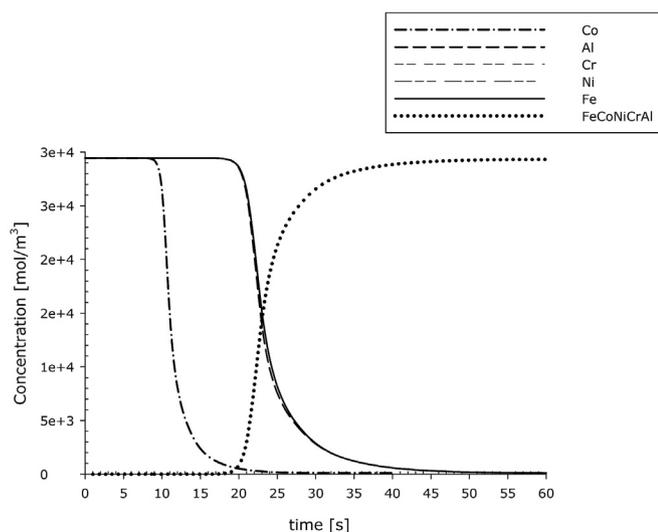


Fig. 6. Simulated the variation of element concentration.

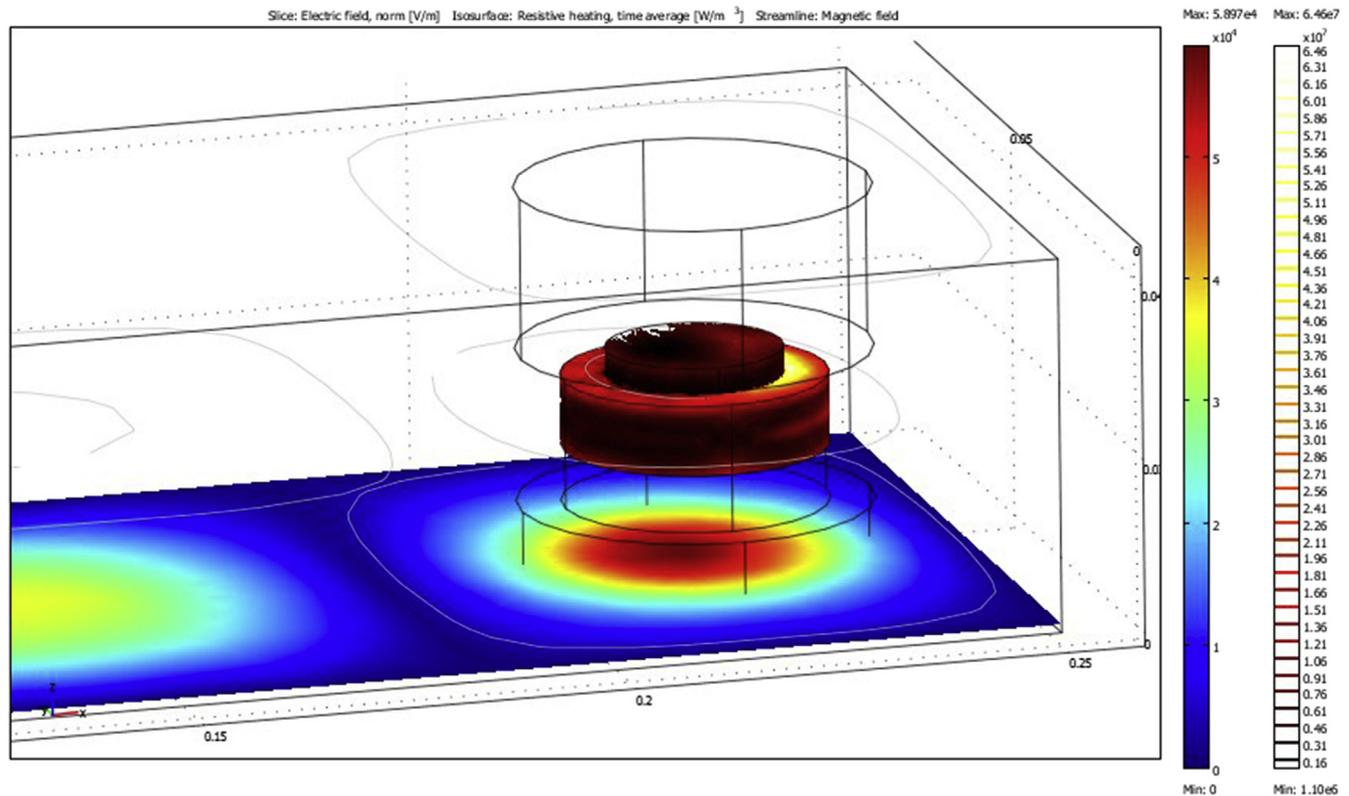


Fig. 7. Resistive Heating (in the precursors disc and SiC element) and Electric Field distribution (at the bottom).

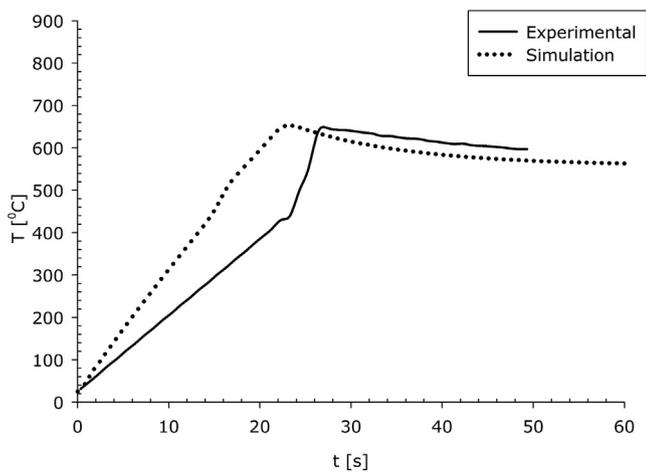


Fig. 8. Experimental and simulated sintering curve.

heat treatment.

3.4. Mechanical properties: hardness and elastic modulus

The mechanical properties of HEA were measured by instrumented indentation (Fig. 12 and Fig. 13) and microhardness test (Fig. 14). Both hardness and elastic modulus of microwave-processed samples (which resulted very similar, independently on the type of powders used, and hence only the average value is shown) are lower than SPS-ed samples, and this can be ascribed to the much higher porosity of the former ones. Fig. 14 reported the

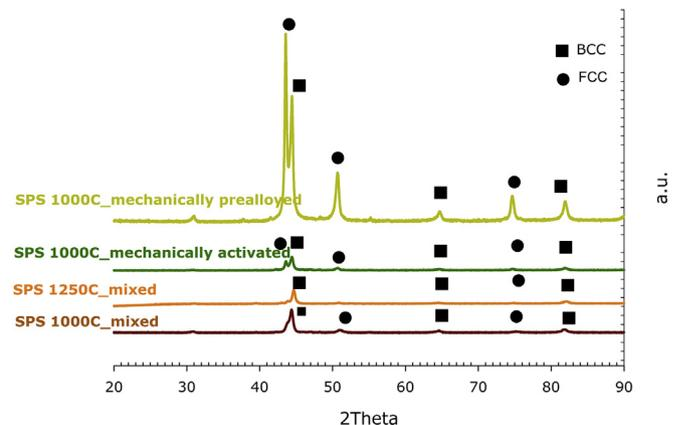


Fig. 9. X-ray diffraction pattern of SPS-processed HEA obtained by mixed powders or mechanically activated powders without post heat treatment.

result of HV and E obtained by instrumental indentation on the two areas at different chemical composition.

The results are in agreement with literature results concerning the same alloy obtained [25,28].

4. Conclusion

In this work the field assisted powder metallurgy route of producing HEAs at equimolar composition of Al,Cr,Ni,Co and Fe, starting from metal powders, was investigated. Both mixed, mechanically activated and mechanically alloyed powders have been

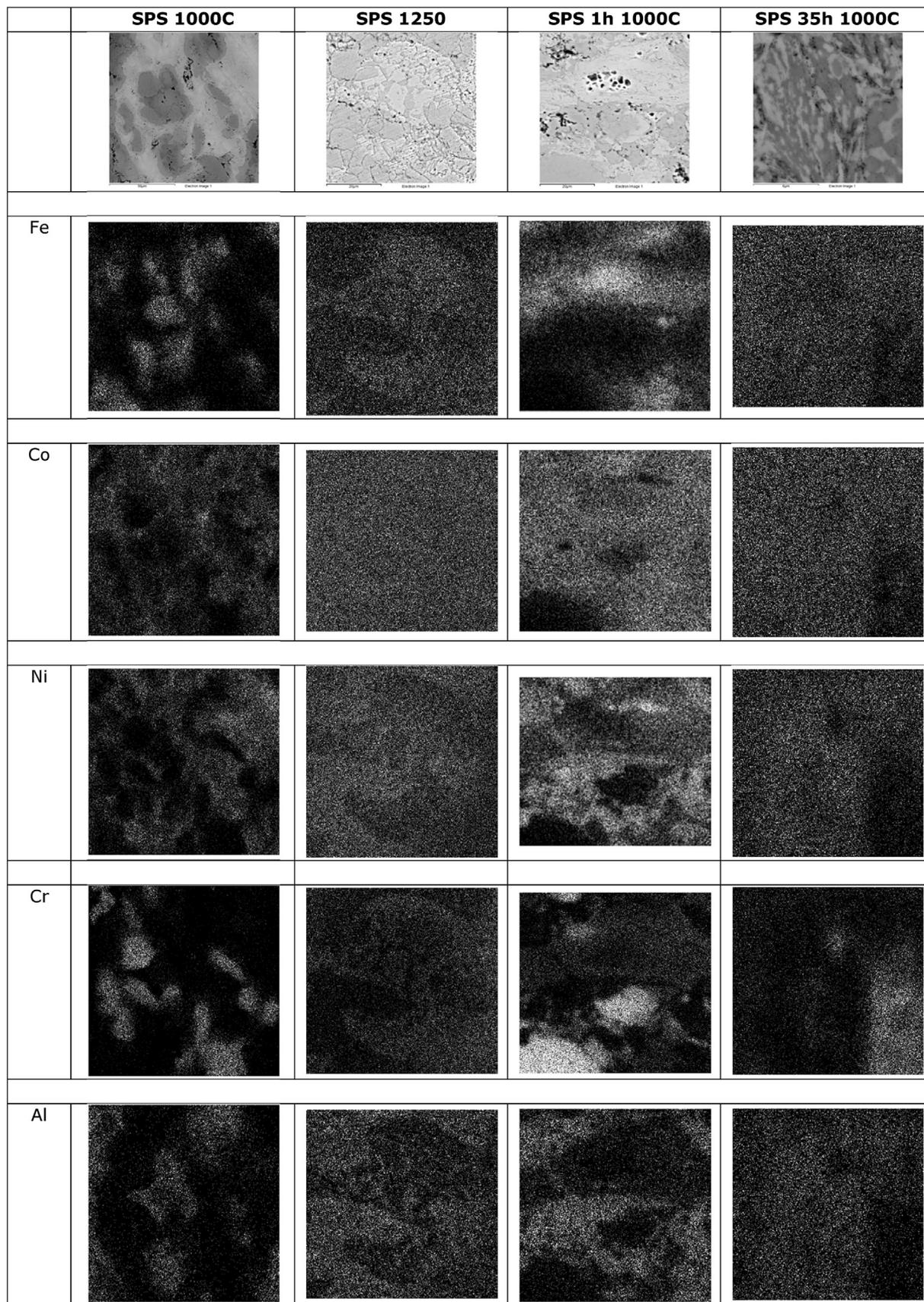


Fig. 10. Element Maps after sintering of SPS samples.

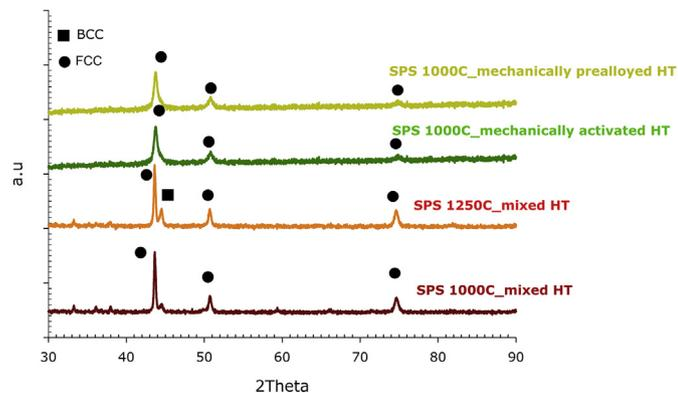


Fig. 11. X-ray diffraction pattern of SPS-processed HEA obtained by mixed powders or mechanically activated powders with post heat treatment (HT).

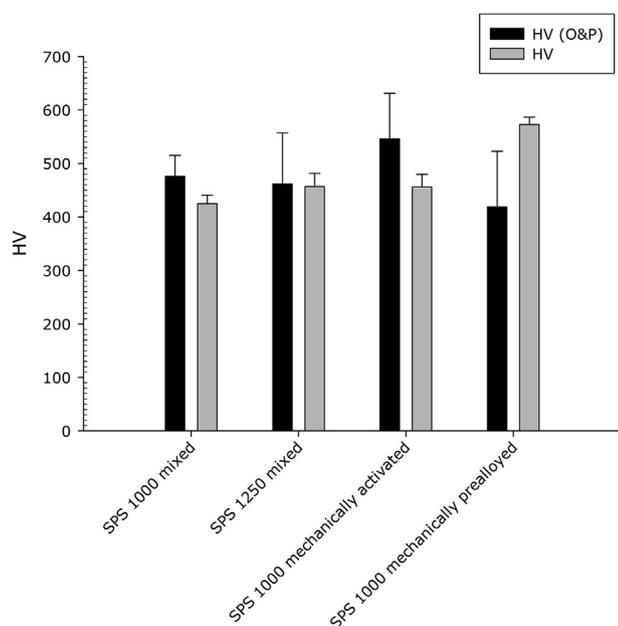


Fig. 12. Equivalent Vickers hardness (HV O&P) and HV1 for the field assisted sintered samples.

used.

The investigated field assisted sintering techniques, namely microwave heating and SPS, allowed an extremely short alloying time, high energy density on the load and negligible contamination by the surrounding environment. Both the conducted sintering-synthesis technology resulted not definitive to produce chemical homogeneity and to obtain a single stable FCC structure. This has been ascribed to the low interdiffusion rate of elements, accompanied by extremely short time of permanence at high temperature, hindering diffusion. In case of microwave heating, numerical simulation demonstrated also that heat generation occurs volumetrically in the load, but not homogeneously, further affecting homogeneity. The post heat treatment (50 h at 1200 °C) allowed to extend the interdiffusion process, leading to a single crystalline structure (FCC), the material being fully recrystallized. After heat treatment samples are isomorphic: they exhibit two different phases with the same FCC cell, but different chemical composition, in detail Fe-Cr richer and Al-Ni richer. SPS-ed samples present a

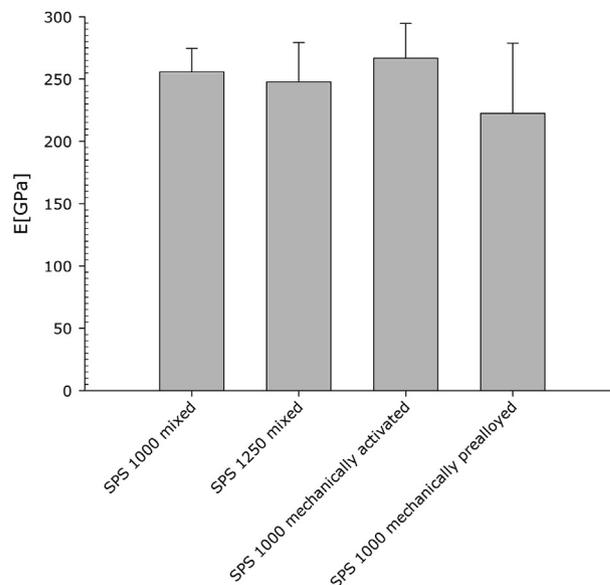


Fig. 13. Elastic modulus as determined from nanoindentation tests for the field assisted sintered samples.

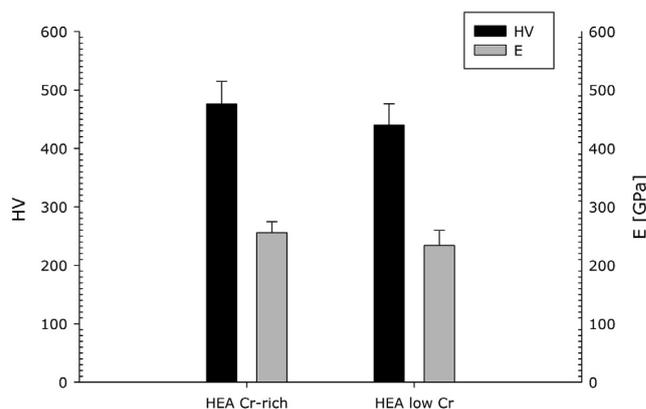


Fig. 14. Elastic modulus and Equivalent Vickers hardness (HV O&P) as determined from nanoindentation tests for the field assisted sintered samples on the two different compositional phase with the same crystallographic structure (FCC).

reduced porosity, while microwave processed ones are much more porous and this is reflected in the mechanical properties.

References

- [1] J.W. Yeh, et al., Nanostructured high-entropy alloys with multiple principal elements: novel alloy design concepts and outcomes, *Adv. Eng. Mater* 6 (2004) 299–303.
- [2] B. Cantor, et al., Microstructural development in equiatomic multicomponent alloys, *Mater. Sci. Eng. A* 375–377 (2004) 213–218.
- [3] Liu, et al., Effects of Sn element on microstructure and properties of $\text{Sn}_x\text{Al}_{2.5}\text{FeCoNiCu}$ multi-component alloys, *J. alloy Compd.* 654 (2016) 327–332.
- [4] D.B. Miracle, O.N. Senkov, A critical review of high entropy alloys and related concepts, *Acta Mater.* 122 (2017) 448–511.
- [5] J.W. Yeh, Industrial development of high-entropy alloys, *Ann. Chim-Sci Mat.* 31 (2006) 633–648.
- [6] J.W. Yeh, et al., Nanostructured high-entropy alloys with multiple principal elements: novel alloy design concepts and outcomes, *Adv. Eng. Mater* 6 (2004) 299–303.
- [7] Y.F. Kao, et al., Microstructure and mechanical property of as-cast, -homogenized, and -deformed $\text{Al}_x\text{CoCrFeNi}$ ($0 \leq x \leq 2$) high-entropy alloys, *J. Alloys Compd.* 488 (2009) 57–64.
- [8] M.G. Poletti, et al., Development of a new high entropy alloy for wear

- resistance: FeCoCrNiW_{0.3} and FeCoCrNiW_{0.3} + 5 at.% of C, Mater. Des. 115 (2017) 247–254.
- [9] O.N. Senkov, et al., Mechanical properties of Nb₂₅Mo₂₅Ta₂₅W₂₅ and V₂₀Nb₂₀Mo₂₀Ta₂₀W₂₀ refractory high entropy alloys, Intermetallics 19 (2011) 698.
- [10] E.D. Tabachnikova, et al., Mechanical properties of the CoCrFeNiMnVx high entropy alloys in temperature range 4.2–300 K, J. Alloys Compd. 698 (2017) 501–509.
- [11] B. Gludovatz, et al., A fracture-resistant high entropy alloy for cryogenic applications, Science 345 (2014) 1153–1158.
- [12] Y.F. Kao, et al., Electrochemical passive properties of Al_xCoCrFeNi (x = 0, 0.25, 0.50, 1.00) alloys in sulfuric acids, Corros. Sci. 52 (2010) 1026–1034.
- [13] R. Wang, et al., Evolution of microstructure, mechanical and corrosion properties of AlCoCrFeNi high entropy alloy prepared by direct laser fabrication, J. Alloys Compd. 694 (2017) 971–981.
- [14] Y. Zhang, et al., Microstructures and properties of high-entropy alloys, Prog. Mat. Sci. 61 (2014) 1–93.
- [15] R. Sriharitha, et al., Phase formation in mechanically alloyed Al_xCoCrCuFeNi (x = ¼ 0.45, 1, 2.5, 5 mol) high entropy alloys, Intermetallics 32 (2013) 119–126.
- [16] J. Joseph, et al., Comparative study of the microstructures and mechanical properties of direct laser fabricated and arc-melted Al_xCoCrFeNi high entropy alloys, Mater. Sci. Eng. A 633 (2015) 184–193.
- [17] P.P. Bhattacharjee, et al., Microstructure and texture evolution during annealing of equiatomic CoCrFeMnNi high-entropy alloy, J. Alloys Compd. 587 (2014) 544–552.
- [18] T.T. Shun, Y.C. Du, Age hardening of the Al_{0.3}CoCrFeNi_{0.1} high entropy alloy, J. Alloys Compd. 478 (2009) 269–272.
- [19] S. Singh, et al., Decomposition in multi-component AlCoCrCuFeNi high-entropy alloy, Acta Mater. 59 (2011) 182–190.
- [20] Hiroshi Shiratori, et al., Relationship between the microstructure and mechanical properties of an equiatomic AlCoCrFeNi high-entropy alloy fabricated by selective electron beam melting, Mater. Sci. Eng. A 656 (2016) 39–46.
- [21] S. Katakam, et al., Laser assisted high entropy alloy coating on aluminum: microstructural evolution, J. Appl. Phys. 116 (2014), 104906.1–104906.6.
- [22] X.W. Qiu, et al., Microstructure and corrosion resistance of AlCrFeCuCo high entropy alloy, J. Alloys Compd. 549 (2013) 195–199.
- [23] S. Varalakshmi, M. Kamaraj, B.S. Murty, Processing and properties of nanocrystalline CuNiCoZnAlTi high entropy alloys by mechanical alloying, Mater. Sci. Eng. A 527 (2010) 1027–1030.
- [24] P. Veronesi, et al., Microwave Processing of High Entropy Alloys: a Powder Metallurgy Approach, Accepted Chemical Engineering and Processing: Process Intensification, In Press, Corrected Proof, Available online 9, March 2017.
- [25] W. Ji, et al., Mechanical alloying synthesis and spark plasma sintering consolidation of CoCrFeNiAl high entropy alloy, J. Alloys Compd. 589 (2014) 61–66. Y. Liu, et al., Preparation of superfine-grained high entropy alloy by spark plasma sintering gas atomized powder, Intermetallics, 68 (2016) 16–22.
- [26] V. Dolique, et al., Complex structure composition relationship in thin films of AlCoCrCuFeNi high entropy alloy, Mater. Chem. Phys. (2009) 117–142.
- [27] V. Soare, et al., Electrochemical deposition and microstructural characterization of AlCrFeMnNi and AlCrCuFeMnNi high entropy alloy, Appl. Surf. Sci. 358 – B (2015) 533–539.
- [28] S. Mohanty, et al., Powder metallurgical processing of equiatomic AlCoCrFeNi high entropy alloy: microstructure and mechanical properties, Mater. Sci. Eng. A 679 (2 January 2017) 299–313.
- [29] F.J. Baldenebro-Lopez, et al., Simultaneous effect of mechanical alloying and arc-melting processes in the microstructure and hardness of an AlCoFeMoNiTi high-entropy alloy, J. Alloys Compd. 643 (2015) S250–S255.
- [30] G.D. Sathiaraj, et al., The effect of heating rate on microstructure and texture formation during annealing of heavily cold-rolled equiatomic CoCrFeMnNi high entropy alloy, J. Alloys Compd. 688 (2016) 752–761.
- [31] L. Ma, et al., Cooling rate-dependent microstructure and mechanical properties of Al_xSi_{0.2}CrFeCoNiCu_{1-x} high entropy alloys, J. Alloys Compd. 694 (2017) 61–67.
- [32] A. Kumar, M. Gupta, An insight into evolution of light weight high entropy alloys: a review, Metals 6 (2016) 1–19.
- [33] Ji Wei, et al., Mechanical alloying synthesis and spark plasma sintering consolidation of CoCrFeNiAl high-entropy alloy, J. Alloys Compd. 589 (2014) 61–66.
- [34] M. Ornov, et al., Structural evolution of spark plasma sintered AlFeCuCrMg_x (x = ¼ 0, 0.5, 1, 1.7) high entropy alloys, Intermetallics 77 (2016) 46–56.
- [35] J. Wei, et al., Alloying behavior and novel properties of CoCrFeNiMn high-entropy alloy fabricated by mechanical alloying and spark plasma sintering, Intermetallics 56 (2015) 24–27.
- [36] W. Teng, J. Kong, C. Bingxuan, Microstructure and mechanical properties of FeCoNiCuAl high-entropy alloy prepared by microwave-assisted combustion synthesis, Powd. Met. Tech. (2011) 435–438. Chinese.
- [37] P. Veronesi, et al., Microwave-assisted preparation of high entropy alloys, Technologies 3 (2015) 182–197.
- [38] P. Veronesi, et al., Microwave assisted synthesis of Si-modified Mn₂₅FeNi₂₅Cu(50-x) high entropy alloys, Mater. Lett. Vol. 162 (2016) 277–280.
- [39] P. Veronesi, et al., A Microwave assisted combustion synthesis of non-equilibrium intermetallic compounds, J. Micr. Pow. Electr. En. 44 (1) (2010) 46–56.
- [40] R. Rosa, P. Veronesi (Chapter 2), in: N.J. Reynolds (Ed.), Functionally Graded Materials Graded by Combustion Synthesis Techniques: a Review. Functionally Graded Materials, Publisher: Nova Science Publishers, 2012, pp. 93–122.
- [41] E. Colombini, et al., Microwave ignited combustion synthesis as a joining technique for dissimilar materials: modeling and experimental results, Int. J. Self-Prop. High-Temp. Synth. 21 (1) (2012) 25–31.
- [42] R. Rosa, P. Veronesi, C. Leonelli, A review on combustion synthesis intensification by means of microwave energy, Chem. Eng. Proc. Proc. Intens. 71 (2013) 2–18.
- [43] P. Veronesi, et al., Enhanced reactive NiAl coatings by microwave-assisted SHS, Compel 27 (2) (2008) 491–499.
- [44] R. Rosa, et al., Alternative sintering processes: microwave (MW)-Assisted combustion synthesis of micrometric metallic powders for the preparation of intermetallic-based materials, in: European PM Conference Proceedings; European Congress and Exhibition on Powder Metallurgy 1-7. Shrewsbury, The European Powder Metallurgy Association, 2010.
- [45] R. Wanga, et al., Evolution of microstructure, mechanical and corrosion properties of AlCoCrFeNi MPEAs prepared by direct laser fabrication, J. Alloys Compd. 694 (2017) 971–981.
- [46] W.C. Oliver, G.M. Pharr, An improved technique for determining hardness and elastic modulus using load and displacement sensing indentation experiments, J. Mater. Res. 6 (1992) 1564–1583.
- [47] G. Bracq, et al., The fcc solid solution stability in the Co-Cr-Fe-Mn-Ni multi-component system, Acta Mater. 128 (2017) 327–336.
- [48] K.-Y. Tsai, M.-H. Tsai, J.-W. Yeh, Sluggish diffusion in Co-Cr-Fe-Mn-Ni high entropy alloys, Acta Materialia 61 (2013) 4887–4897.
- [49] R. Rosa, et al., Microwave ignition of the combustion synthesis of aluminides and field-related effects, J. Alloys Compd. 657 (2016) 59–67.
- [50] E. Colombini, et al., A Microwave Ignited Combustion Synthesis of Intermetallic Compounds, Modelling and Experimental Results vol. 4, 2011. La Metallurgia Italiana.
- [51] R. Rosa, et al., Microwave ignited combustion synthesis as a joining technique for dissimilar materials, J. Mater. Eng. Perform. JMEPEG 21 (2012) 725–732.
- [52] R.L. Blaine, H.E. Kissinger, Homer kissinger and the kissinger equation, Thermochim. Acta 540 (2012) 1–6.
- [53] H. Kissinger, Reaction kinetics in DTA, Anal. Chem. 29 (11) (1957) 1702–1706.
- [54] Z.A. Munir, U. Anselmi-Tamburini, M. Ohyanagi, The effect of electric field and pressure on the synthesis and consolidation of materials: a review of the spark plasma sintering method, J. Mater. Sci. 41 (2006) 763–777.
- [55] R. Orru, et al., Consolidation/synthesis of Materials by electric current activated/assisted sintering, Mater. Sci. Eng. R-Rep 63 (2009) 127–287.
- [56] T.M. Butler, M.L. Weaver, Oxidation behavior of arc melted AlCoCrFeNi multi-component high-entropy alloys, J. Alloys Compd. 674 (2016) 229–244.
- [57] W. Ji, et al., Mechanical alloying synthesis and spark plasma sintering consolidation of CoCrFeNiAl high-entropy alloy, J. Alloys Compd. 589 (2014) 61–66.
- [58] Y.P. Wang, et al., Microstructure and compressive properties of AlCrFeCoNi high entropy alloy, Mater. Sci. Eng. A 491 (2008) 154–158.
- [59] P. Veronesi, et al., Enhanced reactive NiAl coatings by microwave-assisted SHS, COMPEL - Int. J. Comput. Math. Electr. Electron. Eng. 27 (2) (2008) 491–499.
- [60] W.-R. Wang, et al., Effects of Al addition on the microstructure and mechanical property of Al_xCoCrFeNi high-entropy alloys, Intermetallics 26 (2012) 44–51.